

# Enhanced transmission of light through a circularly structured aperture

Evgeny Popov, Michel Nevière, Anne-Laure Fehrembach, and Nicolas Bonod

Using the differential theory of light diffraction by finite cylindrical objects, we study light transmission through a small circular aperture in a metallic screen with concentric corrugation around the nanohole. Poynting vector maps in the region below the screen show that the field enhancement compared with an unstructured aperture is obtained with corrugation lying on the entrance face of the screen. Corrugation on the exit face leads to a more directional radiation close to the normal to the screen. The spectral dependence of the transmission shows a sharp maximum linked with surface plasmon excitation. © 2005 Optical Society of America

OCIS codes: 240.6680, 050.1220.

## 1. Introduction

After the discovery by Ebbesen *et al.*<sup>1</sup> of extraordinary transmission of light through subwavelength hole arrays, a great theoretical effort has arisen to model light diffraction by, first, periodic slits<sup>2–8</sup> and, second, periodic hole arrays.<sup>9–14</sup> In both cases, the periodicity allows the electromagnetic field to be expanded on a Fourier basis and thus reduces the problem to diffraction by a one- or two-dimensional diffraction grating.<sup>15,16</sup> Such an analysis cannot be applied to a single aperture, a fact that turns out to be of great interest in various domains of science and technology, such as biology and near-field microscopy. Several recent experimental publications were devoted to transmission through single-subwavelength apertures,<sup>17,18</sup> including metal-coated tapered fibers.<sup>19</sup> The experimental results have been interpreted by the classic finite-difference time-domain method<sup>17</sup> or by improvement of the method through a local grid refinement.<sup>20</sup> In the meantime, more-specialized theoretical approaches have been developed,<sup>21–24</sup> which use<sup>21</sup> the multipole technique,<sup>25</sup> Green functions,<sup>22</sup> artificial periodicity,<sup>23</sup>

or a Hertz vector formalism.<sup>24</sup> These rigorous approaches are able to account for the observed phenomena at single apertures and to be used to study the validity and limits of physical approximations such as the Kirchhoff approximation. However, these theories have difficulty in modeling an isolated aperture surrounded by concentric structures on the film's surface. Such structured apertures could be of great importance in coupling incident light into a surface plasmon and thus enhancing the local field in the apertures. It has been suggested, however,<sup>26</sup> that these apertures be used to tighten the light radiated by the aperture. This procedure would be necessary to improve measurement efficiency, because from scalar diffraction theory it can be concluded that unstructured subwavelength holes will diffract light in a cone with an angular aperture exceeding 1 rad.

Taking advantage of our experience with grating theories,<sup>16</sup> we recently developed a differential theory of light diffraction by finite-length cylindrical objects.<sup>27</sup> It represents the electromagnetic field on a Bessel–Fourier basis and reduces the problem to numerical integration of a first-order differential set. This theory has already proved useful in fiber modeling<sup>28</sup> and in the study and optimization of plasmon resonances<sup>29,30</sup> on single or structured apertures. Our aim in this paper is to study the influence of concentric structures on the beam shaping and the intensity of the transmission of light through subwavelength apertures.

## 2. Description of the Problem

Figure 1 represents a plane metallic screen pierced by a cylindrical hole of radius  $R_1$ , together with the notation used and the Cartesian  $(x, y, z)$  and cylin-

E. Popov (e.popov@fresnel.fr), M. Nevière, and A.-L. Fehrembach are with the Institut Fresnel, Unité Mixte de Recherche Associée au Centre National de la Recherche Scientifique 6133, Université de Provence, Faculté des Sciences et Techniques de St. Jérôme, Avenue Escadrille Normandie Niémen, 13397 Marseille Cedex 20, France. N. Bonod is with the Commissariat à l'Energie Atomique, Centre d'Etudes Scientifiques et Techniques d'Aquitaine, B.P. 2, 33114 Le Barp, France.

Received 10 May 2005; revised manuscript received 29 July 2005; accepted 5 August 2005.

0003-6935/05/326898-07\$15.00/0

© 2005 Optical Society of America

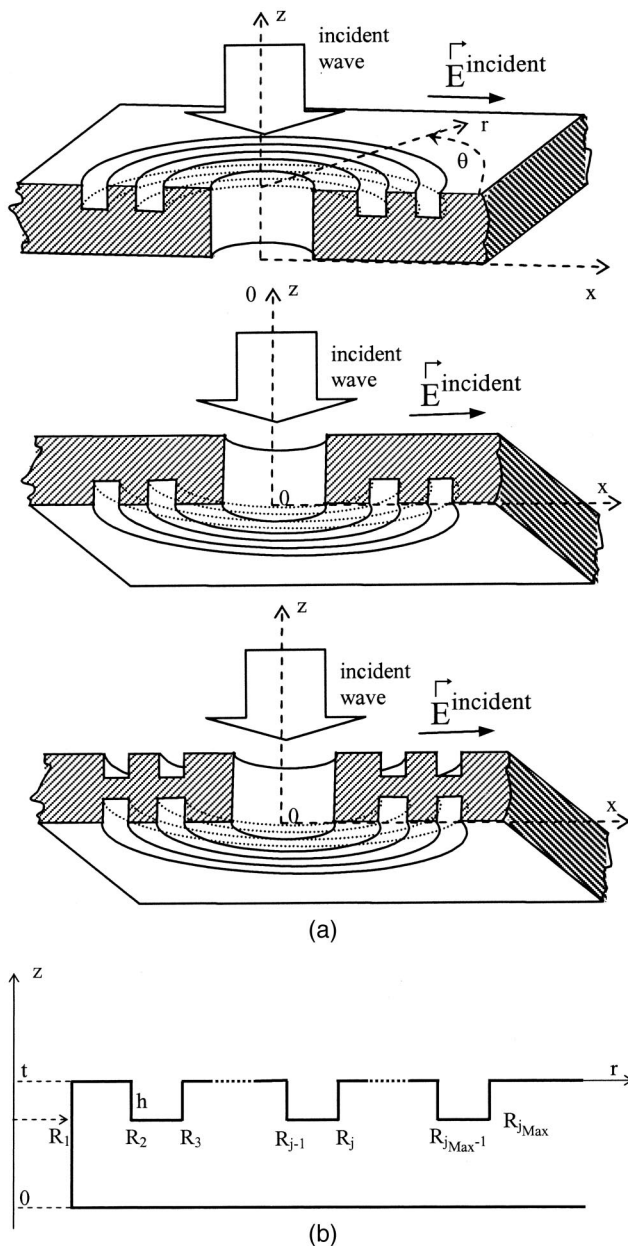


Fig. 1. Schematic representations of the microstructured nanoaperture inside a plane metallic screen. (a) General view of the three systems under study. (b) Cross section of the right-hand side of (a) with definition of groove dimensions.

drical  $(r, \theta, z)$  coordinate systems. The  $z$  axis coincides with the aperture axis, the origin is at the bottom, and the polar angle is  $\theta$ .

The system is illuminated from above at normal incidence with linear polarization along the  $x$  axis by a wave with wavelength  $\lambda$ . The aperture may be surrounded by rectangular-grooved circular concentric corrugation, which can be made on the upper (entrance) or lower (exit) side or on both. In the research described as follows, the screen is made from silver with total thickness  $t = 400$  nm, hole radius  $R_1 = 50$  nm, and a wavelength kept equal to 500 nm, except for Fig. 10 below.

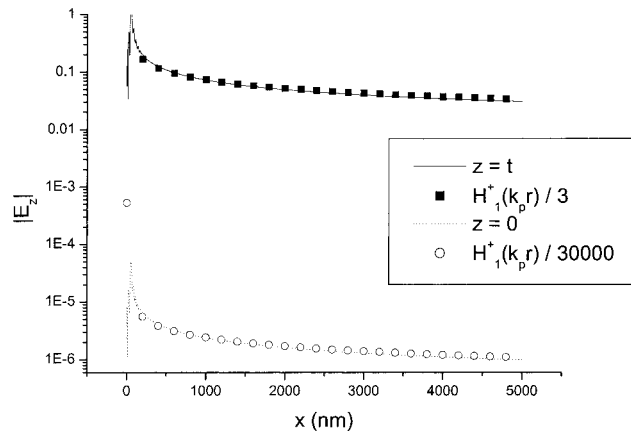


Fig. 2. Dependence on  $x$  of the modulus of the  $z$  component of the electric field diffracted above ( $z = t$ ) and below ( $z = 0$ ) a 50 nm radius circular aperture in a  $t = 400$  nm thick silver layer. Normally incident light is polarized along the  $x$  axis and has wavelength  $\lambda = 500$  nm. The dotted curve, which represents properly normalized Hankel function  $H_1^+(k_p r)$  with  $k_p = 1.068(2\pi/\lambda)$ , corresponds to constant plasmon propagation along the silver–air interface.

As was discussed in detail in Refs. 29 and 30, a single aperture leads to excitation of a surface plasmon propagating along a plane metallic surface away from the aperture edges. Because of the symmetry of the geometry, two plasmons are excited simultaneously on the lower and the upper screen surfaces. Provided that the layer's thickness is sufficient, the coupling between the two plasmons through the layer is quite weak and can be neglected. At wavelength  $\lambda = 500$  nm and a complex optical index of silver equal to  $0.5 + i2.87$ , propagation constant  $k_p$  of the plasmon is  $k_p = 1.068(2\pi/\lambda)$ . In cylindrical coordinates, the plasmon that exits near the origin propagates in accordance with its dependence on a Hankel function.<sup>30–34</sup> In particular, the  $z$  component of the electric field, which is absent in the incident field under normal illumination, is proportional to  $H_1^+(k_p r) \cos(\theta)$  if the incident field is polarized in the  $x$  direction.<sup>30</sup> This fact is illustrated in Fig. 2, which shows the dependence of  $|E_z|$  on  $r$  at the top and bottom surfaces along the  $x$  axis, compared with that of a suitably normalized Hankel function. The plasmon field going away from the aperture is slowly decreasing as  $1/\sqrt{r}$ .

The perturbation approach to plasmon excitation by single or corrugated apertures developed in Ref. 30 enables corrugation geometry to be optimized to more efficiently excite the plasmon on the entry surface and thus on the exit surface. The groove's position and width are defined from the values of  $R_j$  [Fig. 1(b)]. The optimized values for  $\lambda = 500$  nm, as calculated in Ref. 30, are listed in Table 1. In what follows, we use two numbers of grooves: two ( $j = 2–5$ ) and four ( $j = 2–9$ ) grooves.

### 3. Influence of the Corrugation on the Diffraction Pattern

Using the differential theory<sup>27</sup> as a tool, we obtained the spatial distribution of the electric  $\vec{E}$  and

**Table 1. Values of the Corrugation Wall Positions (in nm) Defined in Fig. 1(b) and Optimized to Plasmon Excitation on a Silver-Air Surface at  $\lambda = 500$  nm**

Number of Walls ( $j$ )	Radius of Wall ( $R_j$ )
2	179.4
3	411.7
4	645.4
5	879.4
6	1113
7	1347.8
8	1582
9	1816
10	2051
11	2285.2
12	2517
13	2755.2
14	2985
15	3222.2

magnetic  $\vec{H}$  fields below the film. Although the device has cylindrical symmetry, the linear polarization of the incident light introduces a dependence of the total field and thus of Poynting vector  $\vec{P} = 1/2\vec{E} \times \vec{H}^*$  on  $\theta$ , where the asterisk denotes complex conjugation. The  $z$  component of  $\vec{P}$  is of special interest because its flux determines the transmission factor in measurements with a detector surface perpendicular to the  $z$  axis. To simplify the representations of the three-dimensional distributions, in what follows we present the mean value of  $P_z$  over  $\theta$ , defined as

$$P_{z,\text{mean}}(r, z) = \int_0^{2\pi} P_z(r, \theta, z) d\theta / 2\pi.$$

When this quantity is integrated from 0 to  $r_0$ , it will give the power flux measured by a detector with a radius equal to  $r_0$  and centered in front of the aperture.

Figure 3 shows  $r$ - $z$  maps of  $2\pi P_{z,\text{mean}}$  below apertures structured with zero, two, and four grooves [Figs. 3(a), 3(b), and 3(c), respectively] positioned symmetrically on both the exit and the entrance sides of the film and with groove depth  $h = 40$  nm, for which the effect is optimal, as we show in Section 4 below. The groove structure increases  $P_{z,\text{mean}}$  and, as a consequence, the transmission, by a factor that reaches  $\sim 100$ . In addition, it increases the directivity.

As a consequence the diffracted field decreases less rapidly in the  $z$  direction, as one can observe from Fig. 4, in which the values of  $P_{z,\text{mean}}$  are given along the negative  $z$  axis, normalized at  $z = 0$ . The presence of two or four grooves has the same influence but, as shown in Fig. 3(c), four grooves lead to stronger enhancement. The weaker decrease in the  $z$  direction is linked to a decrease in the transmitted beam's width, as can be observed from Fig. 5, which shows a cut of Figs. 3(a)–3(c) made at  $z = -1000$  nm and represents

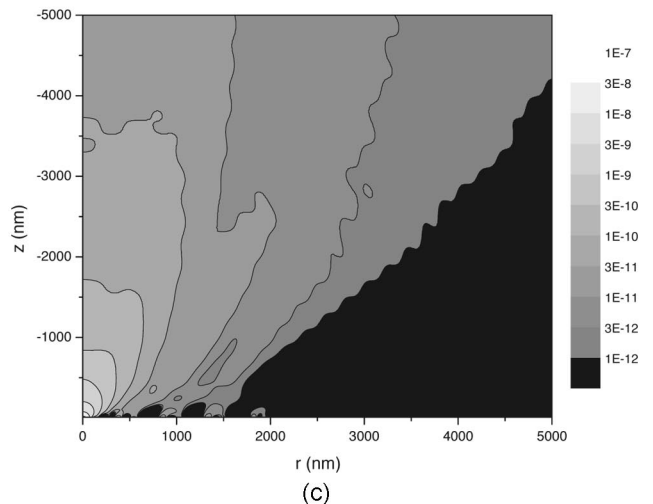
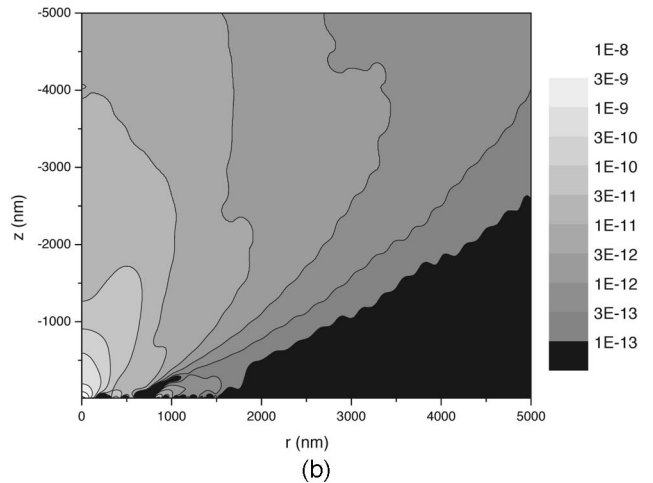
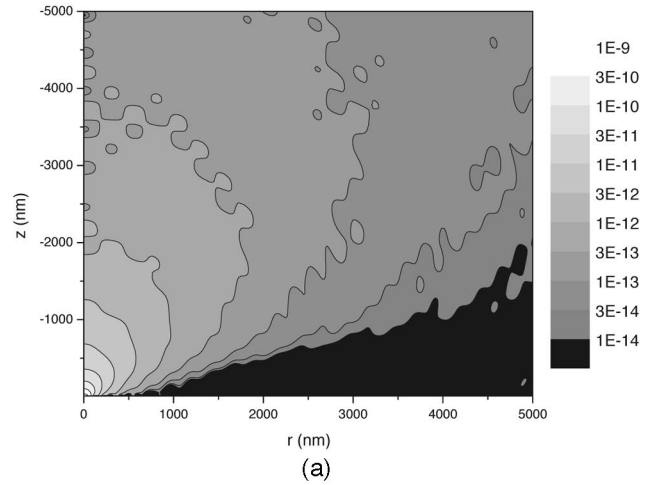


**Fig. 3. Maps of  $2\pi P_{z,\text{mean}}$  as a function of  $r$  and  $z$  for an aperture with  $R_1 = 50$  nm with two-sided corrugation, as shown in the lowest part of Fig. 1(a), and including (a) no grooves, (b) two grooves, and (c) four grooves. Silver layer with optical index equal to  $0.5 + i2.87$ ; total layer thickness,  $t = 400$  nm; groove depth,  $h = 40$  nm; wavelength,  $\lambda = 500$  nm.**

the values of  $P_{z,\text{mean}}(r)$  normalized at  $r = 0$ . The curves clearly show the beam shaping that results from the corrugation. It is necessary to point out that

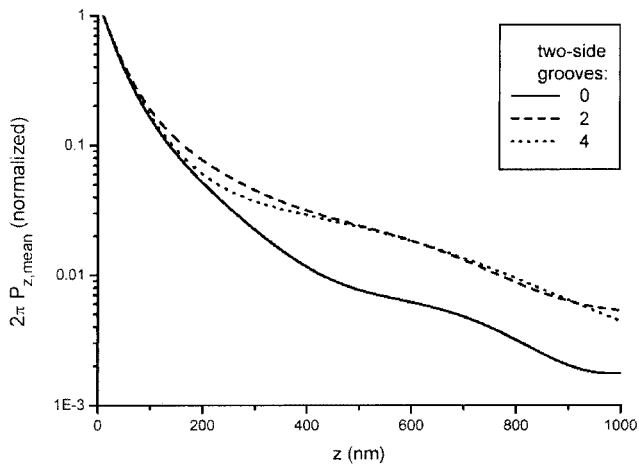


Fig. 4. Decrease of  $2\pi P_{z,\text{mean}}$  along the negative part of the  $z$  axis for the device with two-sided corrugation as described in Fig. 3.

the narrowing of the diffracted beam does not violate the law of diffraction of physical optics. Indeed, this narrower beam is radiated from the entire corrugated area, which is much larger than the single hole.

The last remark is now confirmed, as we determine the influence of the corrugation on the entrance and on the exit metal surfaces, considered separately. Figure 6 shows the same results as in Fig. 3(c), but here the four-groove corrugation is put on the exit (lower) side only, as drawn in the middle part of Fig. 1(a). The same beam shaping is observed as for two-sided corrugation [Fig. 3(c)], but the field magnitude is not enhanced compared with that of a bare hole [Fig. 3(a)]. The explanation for this fact is that the field radiates from a larger surface than the bare hole, but the entrance surface is not changed, and thus the magnitude of both is almost the same. The entrance (upper) face corrugation, however, is supposed to gather (concentrate) the incident field better and thus to increase the field's magnitude, as is clearly visible from Fig. 7, which represents the map

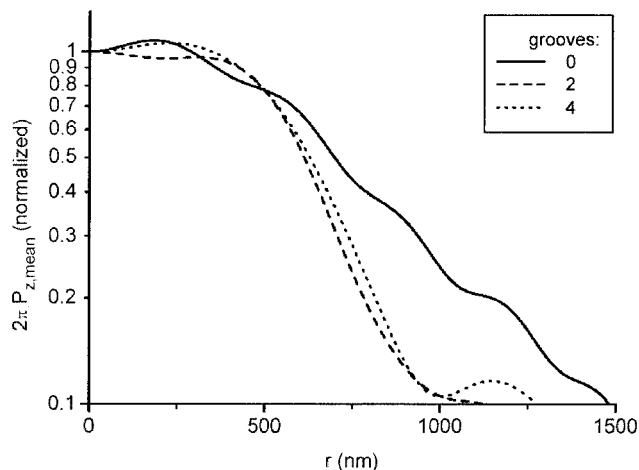


Fig. 5. Decrease of  $2\pi P_{z,\text{mean}}$  as a function of  $r$ , calculated at  $z = -1 \mu\text{m}$ , for the device with two-sided corrugation as described in Fig. 3.

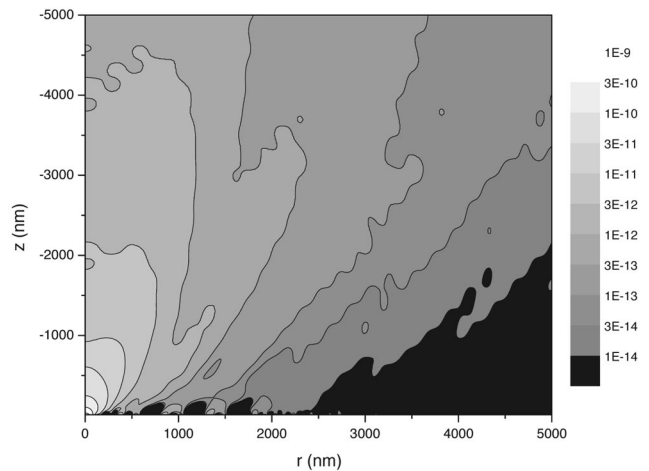


Fig. 6. Map of  $2\pi P_{z,\text{mean}}$  as a function of  $r$  and  $z$  for a four-groove corrugation made on the exit face only, as shown in the middle part of Fig. 1(a). The optogeometrical parameters are the same as in Fig. 3.

of  $2\pi P_{z,\text{mean}}$  for the four-groove system drawn in the upper part of Fig. 1(a). Here the field's magnitude compared with that of Fig. 3(a) is increased by a factor of almost 20, and no beam tightening is seen because the emitting surface is limited by the hole itself.

These conclusions are consistent with the results obtained in the microwave spectral domain,<sup>35</sup> where the screen is considered perfectly conducting.

#### 4. Dependence of the Transmission on Groove-Depth and Wavelength

From our experience with gratings, we know that the field enhancement that is due to plasmon excitation in metallic gratings is characterized by the existence of an optimal groove depth that leads to the strongest plasmon excitation.<sup>36,37</sup> This groove depth is typically of the order of one tenth of the

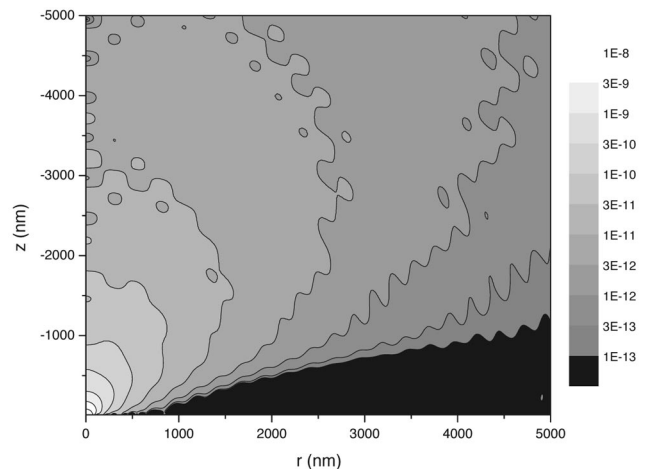


Fig. 7. Map of  $2\pi P_{z,\text{mean}}$  as a function of  $r$  and  $z$  for a four-groove corrugation made on the entrance face only, as shown in the top part of Fig. 1(a). The optogeometrical parameters are the same as in Fig. 3.

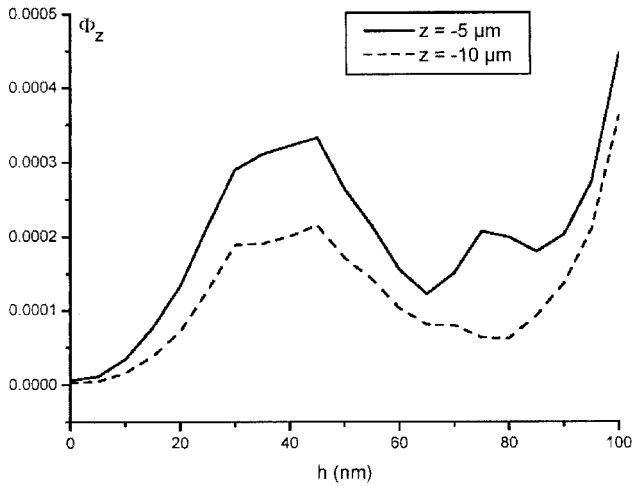


Fig. 8. Power flux transmitted through a horizontal circle with  $5\ \mu\text{m}$  radius as a function of groove depth  $h$  for two positions of the circle,  $z = -5$  and  $z = -10\ \mu\text{m}$ . Two-sided four-groove corrugation with the radii listed in Table 1; total thickness,  $t = 400\ \text{nm}$ ; aperture radius,  $50\ \text{nm}$ .

grating period or of the wavelength or both. Deeper grooves perturb the plasmon propagation and even can completely stop it as a result of strong radiation. A similar phenomenon can be expected for the case studied here. Indeed, one can observe such behavior from Fig. 8. We investigated the influence of the double-faced corrugation [Fig. 1(a), bottom] that had four grooves on each side when groove depth  $h$  was varied but the total film thickness remained unchanged. The figure presents the total flux  $\Phi_z = \int_0^{2\pi} d\theta \int_0^{5\ \mu\text{m}} P_z r dr$  of the Poynting vector through a surface that has a  $5\ \mu\text{m}$  radius and is perpendicular to the  $z$  axis. Whatever the position of the surface below the screen, the dependence on groove depth shows a maximum for  $h \approx 40\ \text{nm}$ , i.e., close to  $\lambda/10$ , which was the reason for our choosing this value in Section 3.

However, when  $h$  grows further, above  $100\ \text{nm}$ , a second region of flux increase is observed. One can understand this by taking into account the fact that the total screen thickness is kept constant. Thus for  $h > 100\ \text{nm}$  the residual screen thickness between the groove bottoms becomes less than  $200\ \text{nm}$ . Then a nonnegligible amount of incident light ( $\lambda = 500\ \text{nm}$ ) is transmitted through the silver film, which adds to the transmittance through the aperture. This reasoning is illustrated in Fig. 9, in which the transmission factor of this two-sided corrugated aperture is compared with the transmission through a plane layer and a single aperture with a radius of  $50\ \text{nm}$ . The transmission factor is defined as the ratio between the flux of the Poynting vector through some surface situated below the aperture and parallel to the layer's surface and the flux of the Poynting vector of the incident wave across an identical surface situated above the aperture. We have chosen for this surface to be represented by a circle with a radius of  $5\ \mu\text{m}$  and centered on the  $z$  axis. The abscissa is equal to

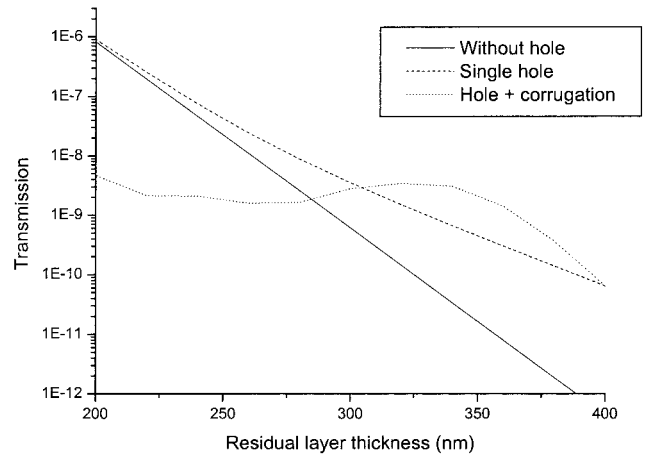


Fig. 9. Comparison of transmission factors for three systems. The transmission factor is equal to transmitted flux  $\Phi$  through a horizontal circle with  $5\ \mu\text{m}$  radius and situated at  $z = -5\ \mu\text{m}$ , normalized by incident flux  $\Phi_i$  through the same circle situated above the aperture. Dotted curve, transmission through two-sided corrugation given in Fig. 8 and presented as a function of the residual thickness of the layer at the groove bottom, equal to  $t - 2h$ . Solid line, transmission through a plane silver layer as a function of layer thickness. Dashed curve, transmission through a single circular aperture with a radius of  $50\ \text{nm}$  in a silver layer, presented as a function of the layer thickness.

the residual layer's thickness,  $t - 2h$ , as measured at the groove bottom, for the corrugated system and to the total layer thickness for the plane layer or for the single aperture. As is now well known, when the layer is sufficiently thick, the aperture transmission can significantly exceed the transmission through the unpierced layer. Below a thickness  $t = 200\ \text{nm}$ , the effect of the aperture is not so prominent, as the direct tunneling through the layer becomes nonnegligible. Because of this enhanced tunneling at small

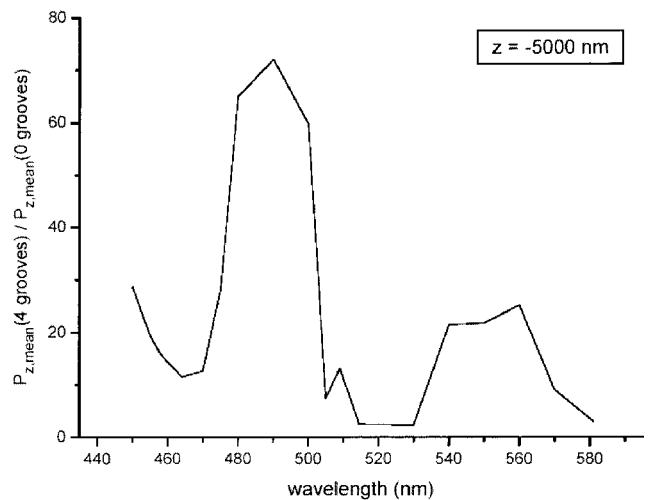


Fig. 10. Spectral dependence of the enhancement factor of the transmittivity for two-sided, four-groove corrugation, sketched in the lowest part of Fig. 1(a) and with groove depth  $h = 40\ \text{nm}$ ; total layer thickness,  $t = 400\ \text{nm}$ ; aperture radius,  $50\ \text{nm}$ ; and groove walls situated according to Table 1.

thicknesses, the effect of the optimized corrugation is more significant for thicker layers.

The resonant nature of the enhancement of the field is clearly visible in the spectral dependence of the effect. Figure 10 shows the variation of the enhancement factor when the wavelength is varied for a two-sided four-groove corrugation with  $h = 40$  nm. The enhancement factor is defined as the ratio of  $P_{z,\text{mean}}$  with the corrugation to  $P_{z,\text{mean}}$  without grooves calculated on the  $z$  axis ( $r = 0$ ) at a distance of  $5 \mu\text{m}$  below the screen. A strong maximum with a value greater than 70 is found at  $\lambda = 485$  nm. This value is quite close to 500 nm, the wavelength for which the position and the width of the grooves have been optimized to resonantly excite the plasmon surface wave.

## 5. Conclusions

This numerical study of diffraction of light by a sub-wavelength aperture in a metallic screen surrounded by concentric surface corrugation shows that entrance-face corrugation can enhance the field transmittance by the aperture, while corrugation on the exit surface can decrease the radiated beam's divergence. By using only a few shallow grooves we achieved an enhancement factor of 70, compared with a bare unstructured aperture.<sup>38</sup>

## References

1. T. W. Ebbesen, H. J. Lezec, H. F. Ghaemi, T. Thio, and P. A. Wolff, "Extraordinary optical transmission through subwavelength hole arrays," *Nature* **391**, 667–669 (1998).
2. U. Schröter and D. Heitmann, "Surface-plasmon-enhanced transmission through metallic gratings," *Phys. Rev. B* **58**, 15,419–15,421 (1998).
3. M. M. J. Treacy, "Dynamical diffraction in metallic optical gratings," *Appl. Phys. Lett.* **75**, 606–608 (1999).
4. J. A. Porto, F. T. Garcia-Vidal, and J. B. Pendry, "Transmission resonances on metallic gratings with very narrow slits," *Phys. Rev. Lett.* **83**, 2845–2848 (1999).
5. T. Lopez-Rios, D. Mendoza, J. J. Garcia-Vidal, J. Sanchez-Dehesa, and B. Pannetier, "Surface shape resonances in lamellar metallic gratings," *Phys. Rev. Lett.* **81**, 665–668 (1998).
6. Ph. Lalanne, J. P. Hugonin, S. Astilean, M. Palamaru, and K. D. Möller, "One-mode model and Airy-like formulae for one-dimensional metallic gratings," *J. Opt. A Pure Appl. Opt.* **2**, 48–51 (2000).
7. M. M. J. Treacy, "Dynamical diffraction explanation of the anomalous transmission of light through metallic gratings," *Phys. Rev. B* **66**, 195105 (2002).
8. Q. Cao and Ph. Lalanne, "Negative role of surface plasmons in the transmission of metallic gratings with very narrow slits," *Phys. Rev. Lett.* **88**, 057403 (2002).
9. H. F. Ghaemi, T. Thio, D. E. Grupp, T. W. Ebbesen, and H. J. Lezec, "Surface plasmons enhance optical transmission through subwavelength holes," *Phys. Rev. B* **58**, 6779–6782 (1998).
10. E. Popov, M. Nevière, S. Enoch, and R. Reinisch, "Theory of light transmission through subwavelength periodic hole arrays," *Phys. Rev. B* **62**, 16,100–16,108 (2000).
11. S. Enoch, E. Popov, M. Nevière, and R. Reinisch, "Enhanced light transmission by hole arrays," *J. Opt. A Pure Appl. Opt.* **4**, S83–S87 (2002).
12. L. Martin-Moreno, F. J. Garcia Vidal, H. J. Lezec, K. M. Pellerin, T. Thio, J. B. Pendry, and T. W. Ebbesen, "Theory of extraordinary optical transmission through subwavelength hole arrays," *Phys. Rev. Lett.* **86**, 1114–1117 (2001).
13. L. Salomon, F. Grillot, A. Zayats, and F. de Fornel, "Near-field distribution of optical transmission of periodic subwavelength holes in a metal film," *Phys. Rev. Lett.* **86**, 1110–1113 (2001).
14. A. Krishnan, T. Thio, T. J. Kim, H. J. Lezec, T. W. Ebbesen, P. A. Wolf, J. Pendry, L. Martin-Moreno, and J. J. Garcia-Vidal, "Evanescence-coupled surface resonance in surface plasmon enhanced transmission," *Opt. Commun.* **200**, 1–7 (2001).
15. R. Petit, ed., *Electromagnetic Theory of Gratings* (Springer-Verlag, 1980).
16. M. Nevière and E. Popov, *Light Propagation in Periodic Media: Differential Theory and Design* (Marcel Dekker, 2003).
17. L. Yin, V. K. Vlasko-Vlasov, A. Rydh, J. Pearson, U. Welp, S. H. Chang, S. K. Gray, G. C. Schatz, D. B. Brown, and C. W. Kimball, "Surface plasmons at single nanoholes in Au films," *Appl. Phys. Lett.* **85**, 467–469 (2004).
18. A. Degiron, H. L. Lezec, N. Yamamoto, and T. W. Ebbesen, "Optical transmission properties of a single subwavelength aperture in a real metal," *Opt. Commun.* **239**, 61–66 (2004).
19. A. Diez, M. V. Andrés, and J. L. Cruz, "Hybrid surface plasma modes in circular metal-coated tapered fibers," *J. Opt. Soc. Am. A* **16**, 2978–2982 (1999).
20. A. R. Zakharian, M. Mansuripur, and J. V. Moloney, "Transmission of light through small elliptical apertures," *Opt. Express* **12**, 2631–2648 (2004).
21. R. Wannemacher, "Plasmon-supported transmission of light through nanometric holes in metallic thin films," *Opt. Commun.* **195**, 107–118 (2001).
22. F. J. Garcia de Abajo, "Light transmission through a single cylindrical hole in a metallic film," *Opt. Express* **10**, 1475–1484 (2002).
23. T. Vallius, J. Turunen, M. Mansuripur, and S. Honkanen, "Transmission through single subwavelength apertures in thin metal films and effects of surface plasmons," *J. Opt. Soc. Am. A* **21**, 456–463 (2004).
24. S. Guha and G. D. Gillen, "Description of light propagation through a circular aperture using nonparaxial vector diffraction theory," *Opt. Express* **13**, 1425–1447 (2005).
25. Ch. Hafner, *The Generalized Multipole Technique for Computational Electromagnetics* (Artech House, 1990).
26. H. J. Lezec, A. Degiron, E. Devaux, R. A. Linke, L. Martin-Moreno, F. J. Garcia-Vidal, and T. W. Ebbesen, "Beaming light from a subwavelength aperture," *Science* **207**, 820–822 (2002).
27. N. Bonod, E. Popov, and M. Nevière, "Differential theory of diffraction by finite cylindrical objects," *J. Opt. Soc. Am. A* **22**, 481–490 (2005).
28. N. Bonod, E. Popov, and M. Nevière, "Light transmission through a subwavelength microstructured aperture: electromagnetic theory and applications," *Opt. Commun.* **245**, 355–361 (2005).
29. E. Popov, N. Bonod, M. Nevière, H. Rigneault, P.-F. Lenne, and P. Chaumet, "Surface plasmon excitation on a single subwavelength hole in a metallic sheet," *Appl. Opt.* **12**, 2332–2337 (2005).
30. E. Popov, M. Nevière, A.-L. Fehrembach, and N. Bonod, "Optimization of plasmon excitation at structured apertures," *Appl. Opt.* **44**, 6141–6154 (2005).
31. W. C. Chew and L. Gurel, "Reflection and transmission operators for strips or disks embedded in homogeneous and layered media," *IEEE Trans. Microwave Theory Tech.* **36**, 1488–1497 (1988).
32. W. C. Chew, *Waves and Fields in Inhomogeneous Media* (Van Nostrand Reinhold, 1990).
33. V. A. Kosobukin, "Polarization and resonance effects in optical initiation of cylindrical surface-polaritons and periodic structures," *Fiz. Tverd. Tela (Leningrad)* **35**, 884–898 (1993).
34. P. J. Valle, E. M. Ortiz, and J. M. Saiz, "Near field by sub-wavelength particles on metallic substrates with cylindrical

- surface plasmon excitation," *Opt. Commun.* **137**, 334–342 (1997).
35. M. J. Lockyear, A. P. Hibbins, and J. R. Sambles, "Surface-topography-induced enhanced transmission and directivity of microwave radiation through a subwavelength circular metal aperture," *Appl. Phys. Lett.* **84**, 2040–2042 (2004).
36. M. Nevière, "The homogeneous problem," in *Electromagnetic Theory of Gratings*, R. Petit, ed. (Springer-Verlag, 1980), Chap. 5.
37. M. Nevière, E. Popov, R. Reinisch, and G. Vitrant, *Electromagnetic Resonances in Nonlinear Optics* (Gordon & Breach, 2000), and references therein.
38. H. A. Bethe, "Theory of diffraction by small holes," *Phys. Rev.* **66**, 163–182 (1944).